NASA TECHNICAL NOTE

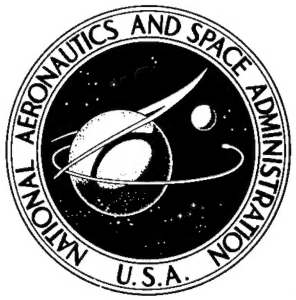

NASA TN D-8417

NASA TN D-8417

MINIMUM-MASS DESIGN OF FILAMENTARY COMPOSITE PANELS UNDER COMBINED LOADS: DESIGN PROCEDURE BASED ON A RIGOROUS BUCKLING ANALYSIS

W. Jefferson Stroud, Nancy Agranoff, and Melvin S. Anderson

Langley Research Center
Hampton, Va. 23665

NATIONAL AERONAUTICS AND SPACE ADMINISTRATION • WASHINGTON, D. C. • JULY 1977

1. Report No. NASA TN D-8417	2. Government Accession No.	3. Recipient's Catalog No.
4. Title and Subtitle MINIMUM-MASS DESIGN OF FILAMENTARY COMPOSITE PANELS UNDER COMBINED LOADS: DESIGN PROCEDURE BASED ON A RIGOROUS BUCKLING ANALYSIS		5. Report Date July 1977 6. Performing Organization Code
7. Author(s) W. Jefferson Stroud, Nancy Agranoff, and Melvin S. Anderson		8. Performing Organization Report No. L-11143 10. Work Unit No. 505-02-42-01
9. Performing Organization Name and Address NASA Langley Research Center Hampton, VA 23665		11. Contract or Grant No. 13. Type of Report and Period Covered Technical Note
12. Sponsoring Agency Name and Address National Aeronautics and Space Administration Washington, DC 20546		14. Sponsoring Agency Code
15. Supplementary Notes		

16. Abstract

A procedure is presented for designing uniaxially stiffened panels made of composite material and subjected to combined inplane loads. The procedure uses a rigorous buckling analysis and nonlinear mathematical programing techniques.

Design studies carried out with the procedure consider hat-stiffened and corrugated panels made of graphite-epoxy material. Combined longitudinal compression and shear and combined longitudinal and transverse compression are the loadings used in the studies. The capability to tailor the buckling response of a panel (i.e., design a panel so that it will have specified buckling loads at various buckling wavelengths) is also explored. Finally, the adequacy of another, simpler, analysis-design procedure is examined.

The report demonstrates that a panel design procedure with a high-quality buckling analysis and with complete generality of constraints is practical. Such a procedure can be used to avoid failure from complex buckling modes and to determine mass and proportions of panels for multiple design load conditions and constraints.

17. Key Words (Suggested by Author(s))	18. Distribution Statement
Stiffened panels Composite structure Structural synthesis Structural efficiency Structural design Minimum-mass design Composite panels	Unclassified – Unlimited Subject Category 39

19. Security Classif. (of this report)	20. Security Classif. (of this page)	21. No. of Pages	22. Price*
Unclassified	Unclassified	40	$4.00

*For sale by the National Technical Information Service, Springfield, Virginia 22161

CONTENTS

MINIMUM-MASS DESIGN OF FILAMENTARY COMPOSITE PANELS UNDER COMBINED LOADS: DESIGN PROCEDURE BASED ON A RIGOROUS BUCKLING ANALYSIS

W. Jefferson Stroud, Nancy Agranoff, and Melvin S. Anderson
Langley Research Center

SUMMARY

A procedure is presented for designing uniaxially stiffened panels made of composite material and subjected to combined inplane loads. The procedure uses a rigorous buckling analysis and nonlinear mathematical programing techniques.

Design studies carried out with the procedure consider hat-stiffened and corrugated panels made of graphite-epoxy material. Combined longitudinal compression and shear and combined longitudinal and transverse compression are the loadings used in the studies. The capability to tailor the buckling response of a panel (i.e., design a panel so that it will have specified buckling loads at various buckling wavelengths) is also explored. Finally, the adequacy of another, simpler, analysis-design procedure is examined.

The report demonstrates that a panel design procedure with a high-quality buckling analysis and with complete generality of constraints is practical. Such a procedure can be used to avoid failure from complex buckling modes and to determine mass and proportions of panels for multiple design load conditions and constraints.

INTRODUCTION

Stiffened panels made of metal and/or composite materials have wide application in aerospace structures. In an effort to increase the structural efficiency of these panels and, at the same time, to account for numerous manufacturing and other design requirements, panels incorporating advanced design concepts are being explored. (See, for example, refs. 1 and 2.) Because these panels exhibit complex buckling modes, it is often necessary to use relatively sophisticated analyses to examine their stability. In recent years, concurrent advances in analysis techniques (see, for example, refs. 3 to 6) and synthesis concepts (see, for example, refs. 7 to 10) have made it possible to develop analysis-design procedures that can cope with the complex buckling modes and, thereby, exploit the potential of the advanced structural design concepts. One such analysis-design procedure is described in this report.

This report presents a procedure for designing uniaxially stiffened panels having an arbitrary cross section, made of composite material, and subjected to inplane longitudinal N_x, transverse N_y, and shear N_{xy} loadings. The procedure is based on a rigorous buckling analysis and nonlinear mathematical programing techniques. Design studies which consider graphite-epoxy hat-stiffened panels and graphite-epoxy corrugated panels are also presented. In these studies, mass-strength charts are developed for panels subjected to combined longitudinal compression and shear and combined longitudinal and transverse compression. The capability to "tailor" the buckling response of a panel (i.e., to design a panel so that it will have specified buckling loads at various buckling wavelengths) is also explored. Finally, the adequacy of a simpler analysis-design procedure (ref. 11) is examined.

SYMBOLS

Values are given in both SI and U.S. Customary Units. The calculations were made in U.S. Customary Units.

A surface area of panel, pL

b_k element lengths defined in figure 8

C constant defined in equation (B1)

D_{16}, D_{26} laminate stiffnesses relating bending behavior with torsional behavior

D_{ij} laminate bending and twisting stiffness matrix

d distance between stiffeners, $2b_4$

E_1, E_2 Young's modulus of composite material in fiber direction and transverse to fiber direction, respectively

EZ1, EZ2, EZ3 eccentricities or offsets in the z-direction shown in figure 19

$F(y_\ell)$ buckling mode shape of panel element in y_ℓ-direction

G_{12} shear stiffness of composite material in coordinate system defined by fiber direction

i,j	integers
K	constant defined in equation (B2)
k	element number
L	panel length in x-direction (see fig. 1)
N_L	required local buckling load for longitudinal compression loading
N_O	required overall buckling load for longitudinal compression loading
N_x	applied longitudinal compressive loading per unit width of panel (see fig. 1)
$N_{x_{cr}}$	value of N_x that causes buckling; may be for specified λ
$\left(N_{x_{cr}}\right)_k$	value of $\left(N_x\right)_k$ that causes local buckling of element k
$\left(N_x\right)_{design}$	value of N_x for which panel is designed
$\left(N_x\right)_k$	longitudinal compressive loading in element k
N_{xy}	applied shear loading per unit width of panel (see fig. 1)
$N_{xy_{cr}}$	value of shear load that causes buckling
$\left(N_{xy_{cr}}\right)_k$	value of $\left(N_{xy}\right)_k$ that causes local buckling of element k
$\left(N_{xy}\right)_k$	shear loading in element k
N_y	applied transverse (y-direction) loading per unit width of panel
n	integer
p	period of stiffened panel, $b_1 + 2b_4$
Re( )	real part of complex quantity within parentheses

t_2 or $t_2(\pm 45)$ thickness of $\pm 45^{o}$ sheet

$t_k(\theta)$ thickness of lamina in element k at fiber orientation angle θ (see fig. 8)

u,v,w buckling displacements (see fig. 17)

W mass of one period of stiffened panel

$\frac{W/A}{L}$ mass index

X,Y,Z axes (defined in figs. 1, 17, and 18)

x,y,z coordinates in longitudinal, transverse, and lateral directions, respectively

y_ℓ, z_ℓ local coordinates for each element making up a panel

α_i design variables; values of the design variables for an arbitrary design

$\bar{\alpha}_i$ values of the design variables at the initial point of a Taylor series expansion

$\epsilon_1^a, \epsilon_2^a, \gamma_{12}^a$ allowable lamina strains in material coordinate system defined by fiber direction

θ fiber orientation angle shown in figure 1

λ buckling half-wavelength, L/n

μ_{12}, μ_{21} Poisson's ratios of composite material in coordinate system defined by fiber direction

ρ density

$\sigma_1^a, \sigma_2^a, \tau_{12}^a$ allowable lamina stresses in material coordinate system defined by fiber direction

Subscripts:

cr	value that causes buckling
k	element number
ℓ	local

A subscript preceded by a comma denotes partial differentiation with respect to the subscript.

ANALYSIS-DESIGN PROCEDURE

The procedure described herein allows a high-quality, eigenvalue buckling analysis to be used to design minimum-mass, uniaxially stiffened panels having an arbitrary cross section and subjected to combined inplane loads (fig. 1). The procedure consists of three basic components:

(1) A linked-plate, eigenvalue buckling analysis for stiffened composite panels. The term "linked-plate" is used in this report to denote the type of buckling analysis used in references 3 to 6.

(2) A nonlinear mathematical programing optimizer for function minimization with inequality constraints.

(3) Approximation concepts such as Taylor series expansions of constraints and selective constraint retention.

These three components and a material strength analysis were combined in a research-oriented computer program to study hat-stiffened and corrugated panels. In this section of the report, the procedure and, in some instances, the computer program that implements the procedure are described. Emphasis is placed on the buckling analysis and on the approximation concepts associated with the buckling constraints. Initial buckling is considered to be a failure mode – that is, it is assumed that the panel has no postbuckling strength. The stress analysis and strength criteria used in the computer program are similar to those used in a panel design procedure described in reference 11.

Loadings Considered

The loadings considered are shown in figure 1. They are:

(1) A uniform, longitudinal compressive loading N_x in the direction of the stiffeners.

(2) A uniform transverse compressive loading N_y.

(3) A uniform shear loading N_{xy}.

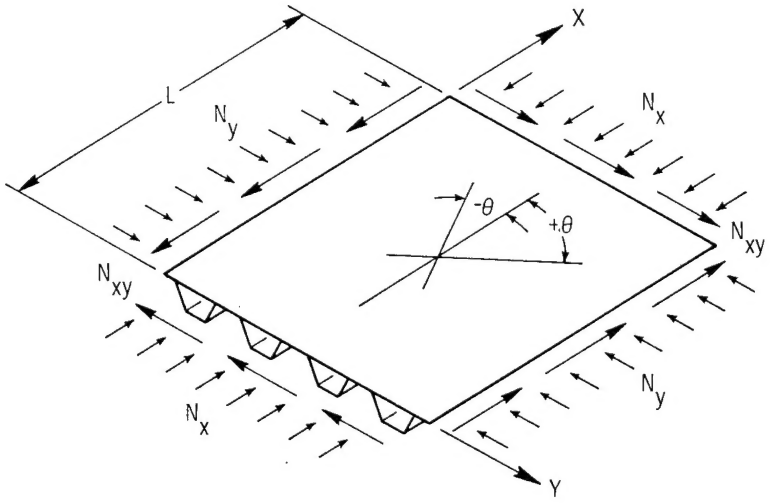

Figure 1.- Loadings considered.

Buckling Analysis

The buckling analysis used in the computer program is an efficient, stiffened-panel buckling analysis code denoted VIPASA (Vibration and Instability of Plate Assemblies including Shear and Anisotrophy) which is described in references 3 and 4. The VIPASA analysis treats an arbitrary assemblage of plates with each plate loaded by N_x, N_y, and N_{xy}. The response of each plate element making up the stiffened panel is obtained using an exact solution of the thin-plate equations. The analysis connects these individual plate elements and maintains continuity of the buckle pattern across the intersection of neighboring plate elements. An illustration of a continuous buckle pattern is shown in figure 2. The stiffened panel is assumed to be uniform in the x-direction (fig. 1) and simply supported along the edges $x = 0$ and $x = L$. For these reasons the buckle patterns in the x-direction are taken to be sine waves whose half-wavelengths are fractions

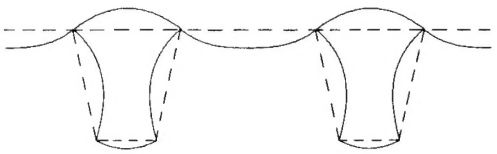

—— — BUCKLING-MODE SHAPE

- - - - - - UNDEFORMED SHAPE

Figure 2.- Continuous buckle pattern.

(1/n) of the panel length. In this report, the type of analysis described above is denoted a "linked-plate" analysis. A more detailed discussion of VIPASA, including comments on the panel modeling used for the hat-stiffened and corrugated panels considered in this report, is presented in appendix A.

Design Procedure

In the panel design procedure described in reference 11, the buckling loads are calculated with relatively simple, explicit equations that require only a small amount of computer time for evaluation. The analysis is, therefore, coupled directly to the optimizer. In contrast, in an analysis such as VIPASA the buckling loads are calculated with an eigenvalue buckling analysis which is much more time-consuming than the explicit equations of reference 11. For that reason, a more sophisticated and efficient sizing technique is employed in the present procedure. The most important feature of the sizing technique is that it is based on a Taylor series approximate analysis approach (refs. 7 and 8). The optimizer, denoted CONMIN (ref. 10), used in the computer program is based on a feasible direction algorithm. In this approximate analysis approach the optimizer uses only approximate values of the constraints based on a sequence of Taylor series expansions of the constraints. The present strategy greatly reduces the number of complete VIPASA analyses required during the synthesis. The general program organization is shown in figure 3.

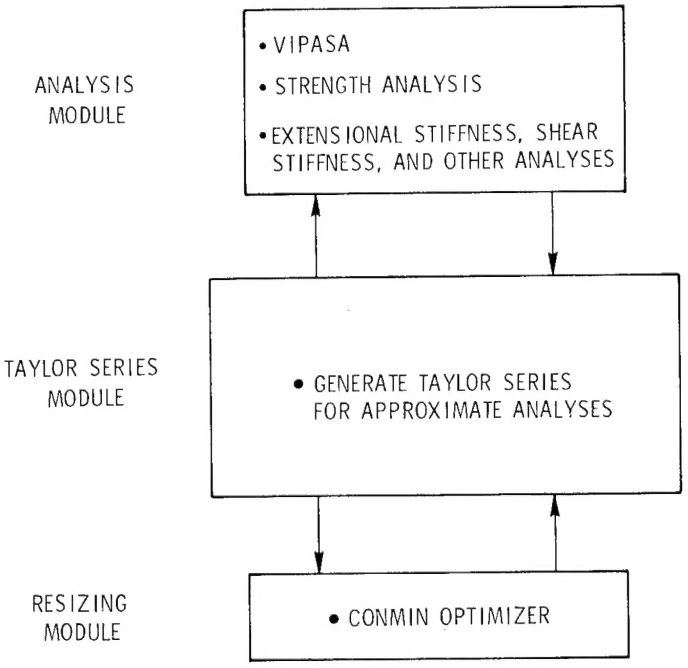

Figure 3.- General approach used in present procedure.

The Taylor series expansions of the constraints are of the form

$$N_{x_{cr}}(\alpha_i) = N_{x_{cr}}(\bar{\alpha}_i) + \sum_i (\alpha_i - \bar{\alpha}_i)\left(\frac{\partial N_{x_{cr}}}{\partial \alpha_i}\right)_{\alpha_i=\bar{\alpha}_i} \tag{1}$$

in which $N_{x_{cr}}$ is the buckling load, α_i are the design variables, and $\bar{\alpha}_i$ are the values of the design variables at the initial point of the expansion. The buckling load at $\bar{\alpha}_i$ and the derivatives of the buckling load at $\bar{\alpha}_i$ are evaluated with VIPASA. (For the studies presented herein, finite-difference approximations were used to calculate the derivatives.) Taylor series expansions are used for the strength constraints as well as for the buckling constraints.

The overall synthesis strategy, which is shown schematically in figure 4, consists of a series of subsyntheses in which the optimizer adjusts the values of the design variables based on approximate values of the constraints (eq. (1)). An upper limit is imposed on the change of each design variable during each subsynthesis to insure the adequacy of both the list of constraints that are considered to be active and the Taylor series expansions of those constraints. These limits to the changes in the design variables are referred to as move limits. The move limits associated with each subsynthesis are indicated by the dashed rectangles in figure 4. (The move limits used in the studies presented herein were usually 10 percent of the values of the design variables at the beginning of a subsynthesis.) The solid circular symbol at the center of each rectangle

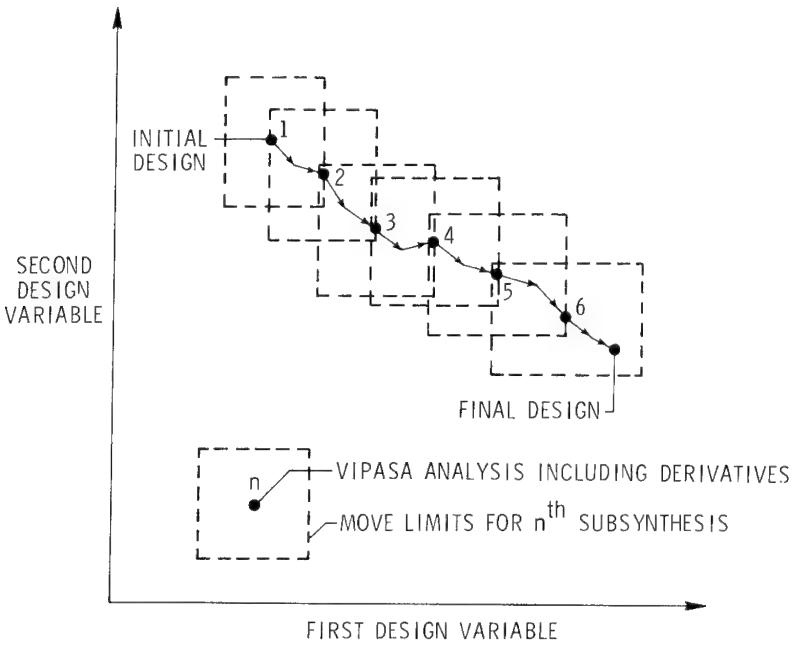

Figure 4.- Synthesis strategy including move limits during subsynthesis in two-design-variable space.

represents the point at which the Taylor series expansions are carried out for each subsynthesis. The end point of one subsynthesis becomes the initial point of the next subsynthesis. Accurate values of the constraints and derivatives of the constraints are then recalculated, and new Taylor series expansions are generated. Ten subsyntheses are usually adequate to obtain convergence if the initial design is reasonably well chosen. (For the studies presented herein, typical run times on Langley's CDC CYBER 175 computer were 100 to 300 seconds for orthotropic panels without shear and 200 to 500 seconds for panels that are anisotropic and/or have a shear loading.)

An example which demonstrates the buckling-constraint aspects of the design problems that must be treated with the procedure is presented in figure 5. In this example a

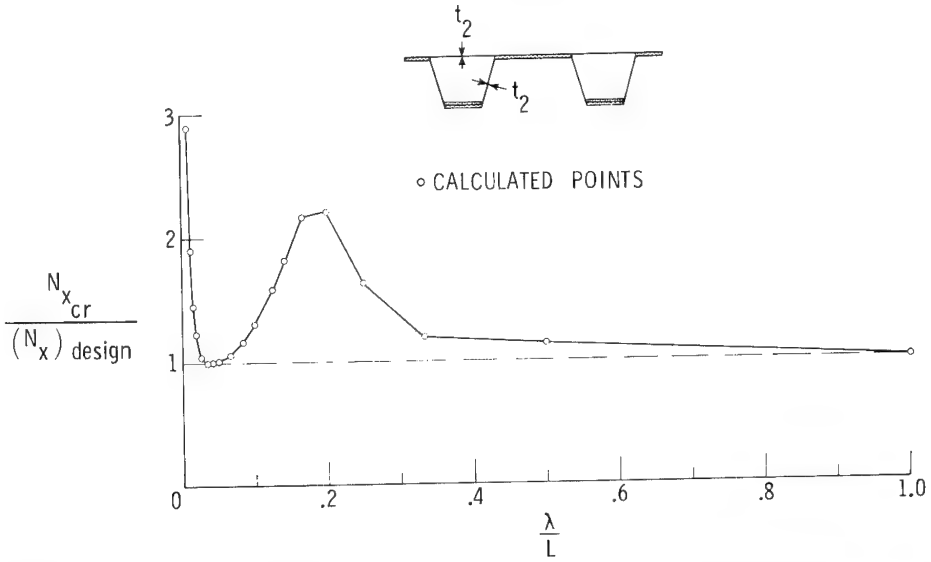

Figure 5.- Ratio of buckling load to design load as a function of buckling half-wavelength for a hat-stiffened panel designed for a loading of N_x/L = 689 kPa (100 lbf/in^2); t_2 = 0.56 mm (0.022 in.).

hat-stiffened panel is designed to support a longitudinal compressive loading of N_x/L = 689 kPa (100 lbf/in^2). The transverse and shear loads are taken to be zero. The buckling response diagram for the final design is shown in figure 5. In this diagram the buckling load is given as a function of the buckling half-wavelength. Both scales are nondimensional for convenience. The object of the design procedure is to insure that the buckling load $N_{x_{cr}}$ is greater than or equal to the design load $(N_x)_{design}$ for all buckling half-wavelengths λ given by λ = L, L/2, L/3, L/4, ... In the case shown in figure 5, the critical half-wavelengths are λ = L, which corresponds to an overall buckling mode, and λ = L/28, which corresponds to a local buckling mode. The buckling-mode shapes for these two buckling modes are given in figures 6 and 7, respectively. In this example, buckling modes corresponding to λ = L/2 and L/3 are near critical; for some cases, these wavelengths became critical at the final design.

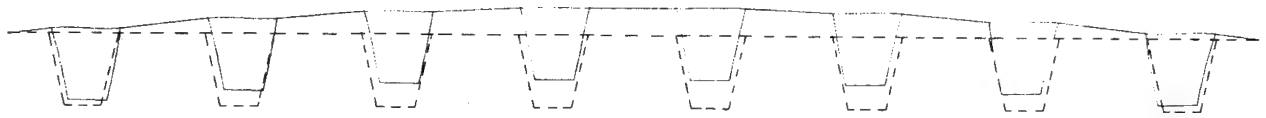

——— BUCKLING-MODE SHAPE

– – – – – UNDEFORMED SHAPE

Figure 6.- Overall-buckling-mode shape for panel whose buckling response diagram is shown in figure 5. $\lambda = L$.

Figure 7.- Local buckling mode shape for panel whose buckling response diagram is shown in figure 5. $\lambda = L/28$.

Buckling at each half-wavelength was considered to be a separate constraint. Only a few of these buckling constraints need to be retained at any stage of the synthesis. The others can be eliminated using various constraint deletion techniques (ref. 8). In the computer program used to obtain the results presented herein, a buckling half-wavelength λ was considered to be active if it was prescribed or if it provided the lowest buckling load at some stage of the synthesis.

Cycling or Mode Switching

There are many buckling eigenvalues at each value of the buckling half-wavelength λ. All of these buckling eigenvalues can be obtained from VIPASA. Although the computer program used to carry out the studies in this report contains sufficient logic to account for several simultaneous buckling eigenvalues at their respective buckling wavelengths, the program examines only one – the lowest – of the buckling eigenvalues at a given wavelength. A second, higher buckling eigenvalue at that same wavelength may have different buckling characteristics and, after a small change in the design, may become the lowest buckling eigenvalue at that same wavelength. Unless buckling eigenvalues with both characteristics are taken into account simultaneously, the procedure may cycle between them and make no progress. Cycling occurred during several of the studies reported herein. (Cycling was controlled by treating one or two of the panel dimensions as fixed parameters rather than as free variables.) An improvement is needed that would identify and provide Taylor series expansions of the critical eigenvalues for more than one buckling mode at the same wavelength.

DESIGN STUDIES

Design studies are presented for panels subjected to two types of loadings: (1) combined longitudinal compression and shear, and (2) combined longitudinal and transverse compression. The capability to tailor the buckling response of a panel and the implications of this tailoring are also explored. In some cases the results of a simpler analysis-design procedure (ref. 11) are given for comparison. Studies which examine the adequacy of the simpler procedure are presented in appendix B. The buckling boundary conditions along the edges $x = 0$ and $x = L$ are simple support, and the boundary conditions along the longitudinal edges (y is constant) are either simple support or symmetric. (The boundary conditions are discussed in more detail in appendix A.)

Configurations

The panel configurations considered are the hat-stiffened and corrugated configurations studied in reference 11 and shown in figures 8(a) and 8(b), respectively. The cross-section geometry is defined in terms of the four dimensions b_1, b_2, b_3, and b_4. The quantities b_1, b_2, and b_3 are the widths of elements 1, 2, and 3, respectively. The quantity b_4 is the half-width of element 4. Because of symmetry, b_4 is replaced by $b_3/2$ in the corrugated panel.

The panels are assumed to be made of a filamentary composite material with ply orientation angle θ measured from a line drawn in the direction of the stiffeners (the x-direction) as shown in figure 1. In the examples presented in this report, only two fiber orientations are considered: $\theta = 0^\circ$ and $\theta = \pm 45^\circ$. The 45° plys are assumed to be balanced and symmetric and are, therefore, denoted $\pm 45^\circ$. For some loadings, in particular those involving a transverse load, the addition of 90° plys may provide more efficient designs; however, 90° plys are not used in the studies presented herein.

The configurations are defined so that the 0° plys and the $\pm 45^\circ$ plys have specific locations (fig. 8(c)). All elements contain $\pm 45^\circ$ plys. Elements 3 and 4 can also contain 0° plys. In both configurations $t_3(0^\circ)$ refers to the thickness of one of the two equal 0° layers in element 3. In the hat-stiffened configuration the thickness of a 0° layer sandwiched between $\pm 45^\circ$ skins in element 4 is denoted $t_4(0^\circ)$.

The hat-stiffened configuration is a uniformly thick corrugated sheet of $\pm 45^\circ$ material attached to an equally thick flat sheet of $\pm 45^\circ$ material with 0° material at specified locations in elements 3 and 4. The corrugated configuration is a uniformly thick corrugated sheet of $\pm 45^\circ$ material with 0° material at specified locations in element 3. In both configurations, the thickness of a $\pm 45^\circ$ sheet is denoted $t_2(\pm 45^\circ)$ or simply t_2.

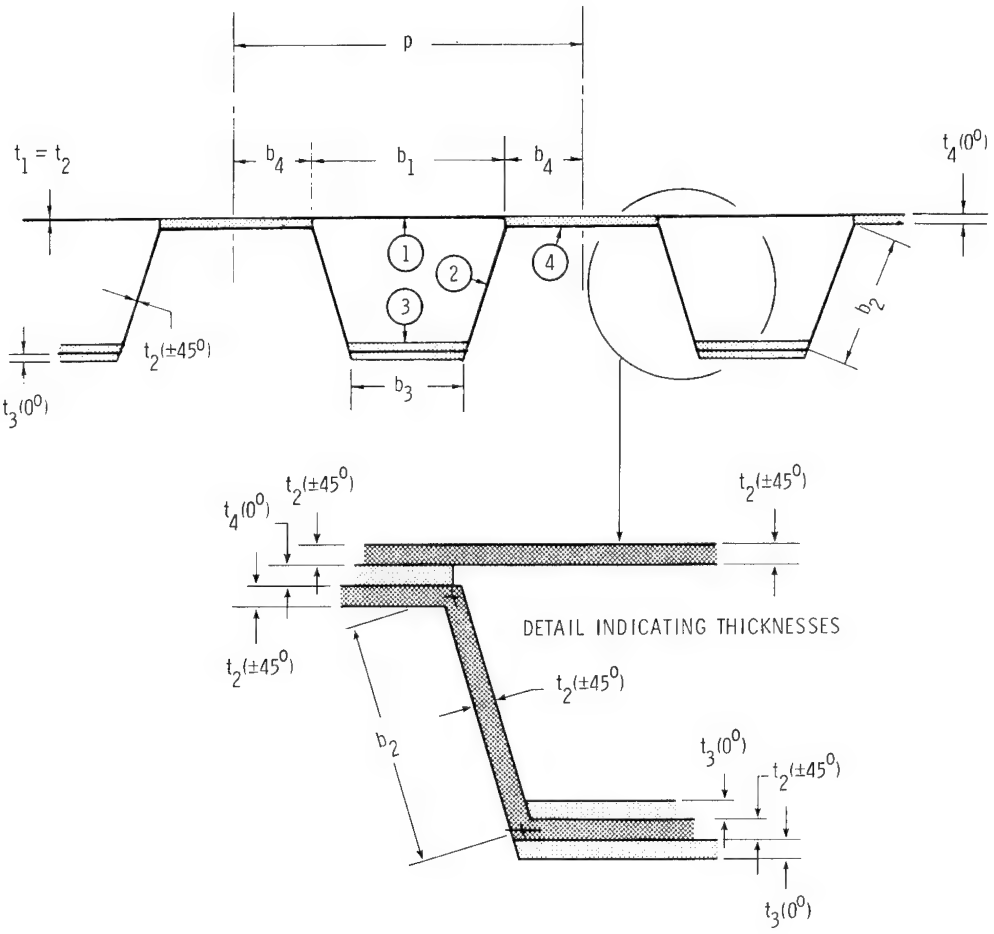

(a) Hat-stiffened panel.

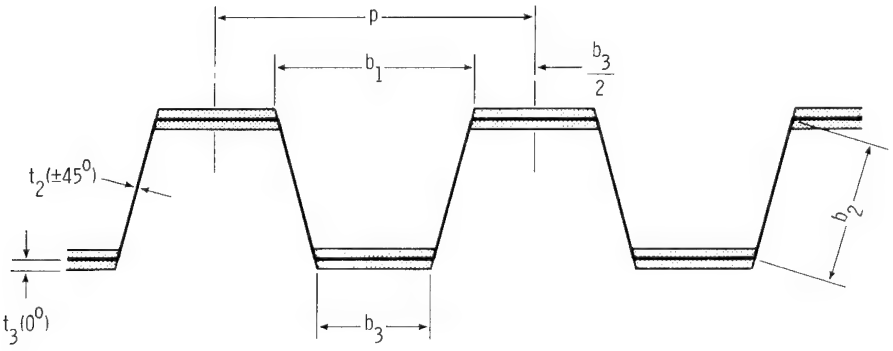

(b) Corrugated panel.

(c) Filament orientation pattern.

Figure 8.- Configurations and design variables. Element identification numbers are indicated in figure 8(a).

The design variables are the thicknesses $t_2(\pm 45^o)$, $t_3(0^o)$, and $t_4(0^o)$, and the lengths b_1, b_2, b_3, and b_4. In all of the studies, the length L of the panel is 0.76 m (30 in.). The upper and lower bounds on the design variables are given in table I, and the material properties used for the studies are given in table II.

Panels Designed for Longitudinal Compression and Shear

Hat-stiffened panels – longitudinal compression and shear.- A structural efficiency diagram for hat-stiffened, graphite-epoxy panels is presented in figure 9. In this diagram

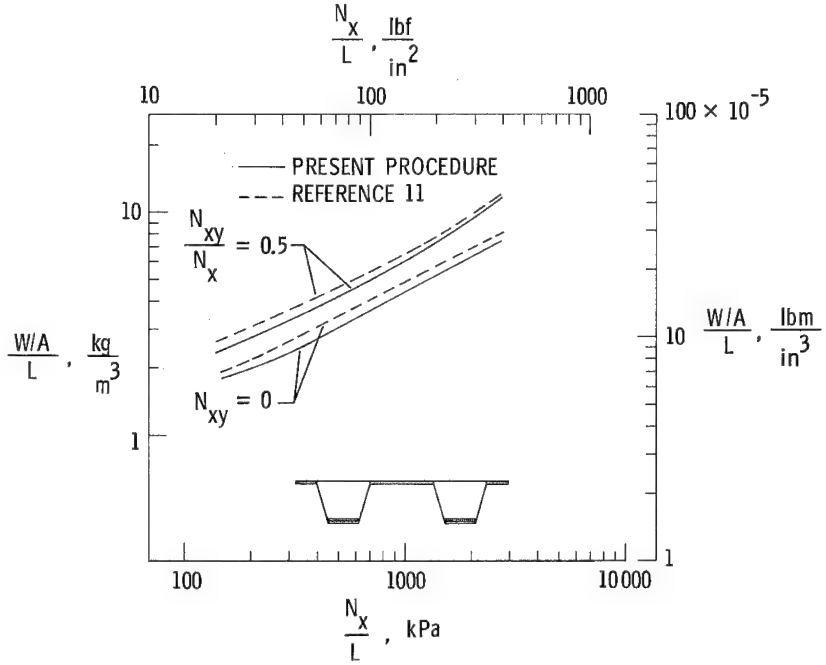

Figure 9.- Structural efficiency of graphite-epoxy, hat-stiffened panels designed for pure longitudinal compression and for longitudinal compression and shear.

the mass index $\frac{W/A}{L}$ of the panels is shown as a function of the loading index N_x/L for two loading cases: (1) pure longitudinal compression and (2) combined longitudinal compression and shear with $N_{xy}/N_x = 0.5$. The solid curves are for panels designed using the present procedure, and the dashed curves are for panels designed using the simplified procedure of reference 11. All design variables vary freely and continuously within the upper and lower bounds given in table I. For these cases, the present procedure provides designs that are up to 14 percent lighter than designs obtained with the simplified procedure presented in reference 11. The panels designed for $N_{xy}/N_x = 0.5$ are about 40 percent heavier than panels designed for N_x only.

Corrugated panels – longitudinal compression and shear.- A structural efficiency diagram for corrugated, graphite-epoxy panels is presented in figure 10. The curve

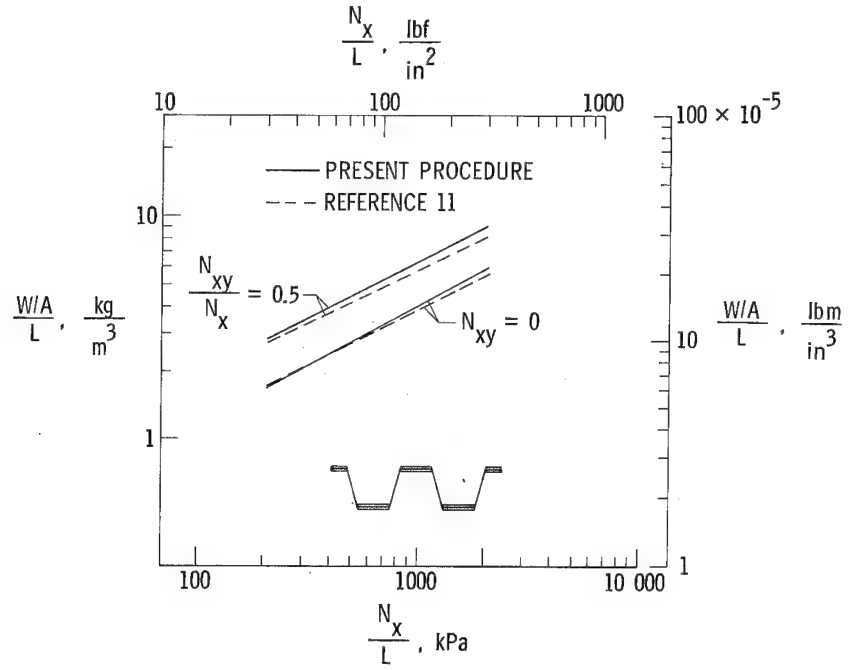

Figure 10.- Structural efficiency of graphite-epoxy corrugated panels designed for pure longitudinal compression and for longitudinal compression and shear.

designations and loadings are similar to those used in figure 9. An important difference between the results for the hat-stiffened panels and the results for the corrugated panels is that for the corrugated panels the dashed curves fall below the solid curves, indicating that the panels designed with the simplified procedure are lighter than the panels designed with the present procedure. However, unlike the hat-stiffened panels, calculations with VIPASA indicate that corrugated panels designed with the simplified procedure do not carry the design load. The adequacy of the simplified analysis is discussed in greater detail in appendix B. The panels designed for $N_{xy}/N_x = 0.5$ are about 60 percent heavier than panels designed for N_x only.

Hat-stiffened panels – longitudinal compression with stiffener spacing requirement.- A common design requirement for stiffened panels is minimum stiffener spacing. The effect of imposing such a requirement is shown in figure 11. The curves are for hat-stiffened, graphite-epoxy panels supporting a longitudinal compressive loading only. In the upper two curves the distance d between stiffeners is equal to 12.7 cm (5.0 in.). In the lower two curves the distance d is allowed to vary freely and is always less than 12.7 cm. The design trends are the same as those presented in reference 11. The mass penalty associated with increasing the stiffener spacing is 30 to 75 percent, depending upon the loading. For the hat-stiffened panels with a spacing requirement of $d = 12.7$ cm the present procedure provides designs that are about 7 percent lighter than the corresponding designs obtained with the simplified procedure of reference 11.

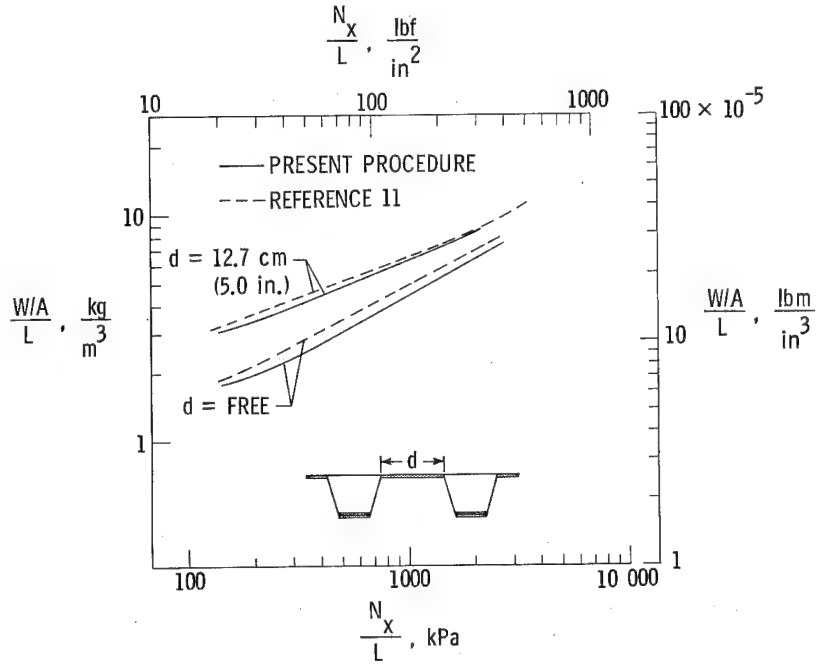

Figure 11.- Structural efficiency of graphite-epoxy, hat-stiffened panels designed for longitudinal compression; with and without constraint on distance d between stiffeners.

Effect of Transverse Compressive Load N_y

The primary inplane loading on a uniaxially stiffened panel is usually a combination of N_x and N_{xy}, where N_x is in the direction of the stiffeners. The structure containing the panel is normally designed so that other structural members carry the major portion of the transverse load N_y. Small transverse loads in a panel cannot, however, be completely eliminated. Studies were carried out with the present procedure to examine the effect of small transverse compressive loads N_y on the load-carrying ability and on the mass of hat-stiffened panels.

In the first study, buckling loads were calculated for a panel designed only for a longitudinal load N_x but subjected to a small transverse load N_y in addition to the N_x load. The design load is N_x/L = 689 kPa (100 lbf/in^2); N_y is 3 percent of N_x. The thickness t_2 is 0.56 mm (0.022 in.). Buckling response diagrams for the panel with and without the transverse loading are given in figure 12. For this panel, the results indicate that with a combined loading of N_x and N_y in which N_y is only 3 percent of N_x, the critical value of N_x is reduced by 28 percent from its value when $N_y = 0$. It is apparent that a small transverse compressive loading N_y can cause a large reduction in the longitudinal buckling load $N_{x_{cr}}$.

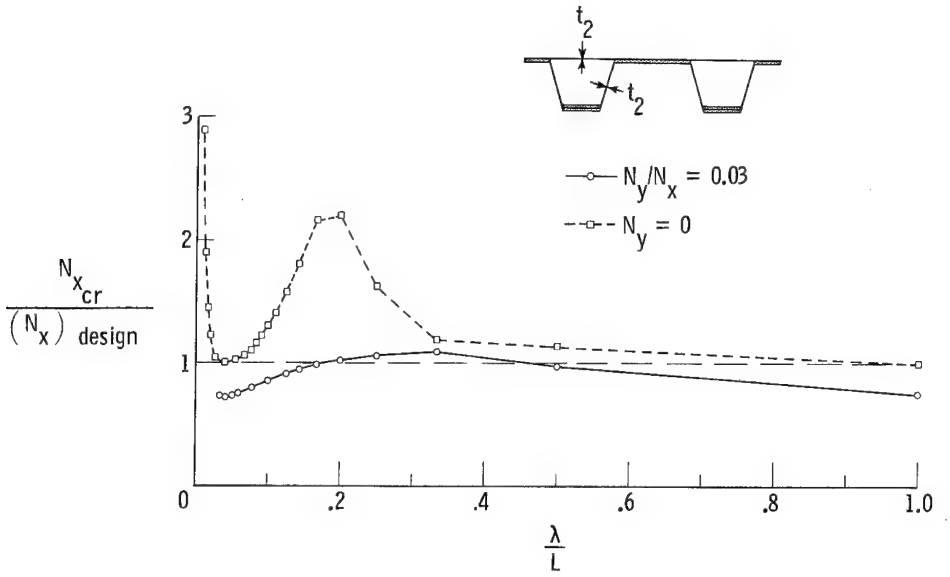

Figure 12.- Ratio of buckling load to design load as a function of buckling half-wavelength for one hat-stiffened panel designed to support a loading of $N_x/L = 689$ kPa (100 lbf/in^2). In the upper buckling response diagram, the loading is the design loading. In the lower diagram, a small transverse loading N_y is added to the design longitudinal loading N_x. $t_2 = 0.56$ mm (0.022 in.).

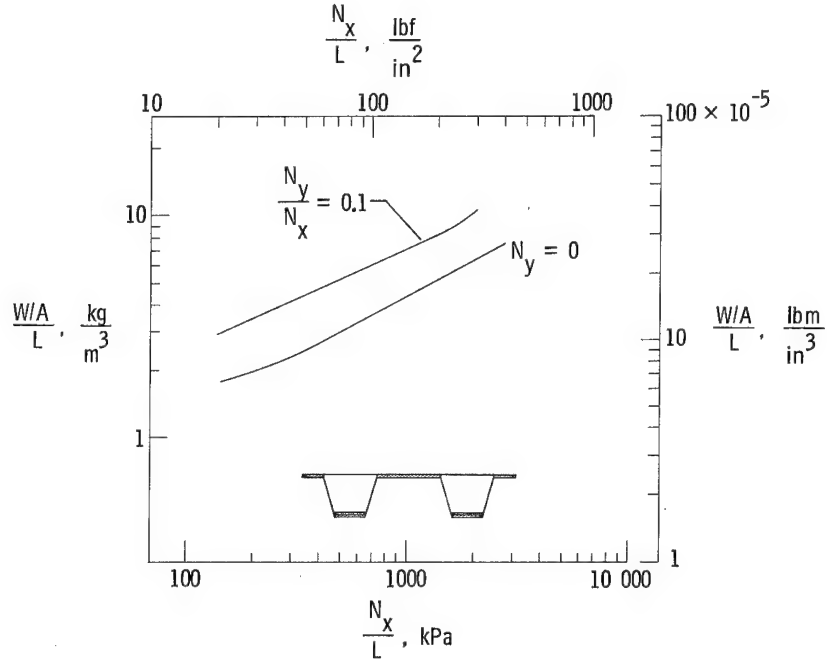

Figure 13.- Structural efficiency of graphite-epoxy, hat-stiffened panels designed for pure longitudinal compression and for longitudinal and transverse compression.

A structural efficiency diagram which shows the increase in mass required to support a transverse loading is presented in figure 13. In the lower curve N_y is equal to zero, and in the upper curve N_y is equal to 10 percent of N_x. In both curves all dimensions, including t_2, vary freely and continuously. For the range of the loading index N_x/L considered, the panels with $N_y/N_x = 0.1$ are about 70 percent heavier than the panels with no transverse load. It is likely that this increase in mass would be diminished if 90^o plys were included in the panel.

Tailoring the Buckling Response of a Panel

In the buckling response diagram presented in figure 5 the buckling load has a relative minimum at $\lambda = L/28$, which corresponds to a local buckling mode, and another low point at $\lambda = L$ which is an overall buckling mode. Other panels in this report have a similar buckling response (one or two short-wavelength buckle modes and one or two longer wavelength buckle modes are active simultaneously) whether designed by the simplified procedure of reference 11 or the present procedure. When additional design requirements such as material strength or extensional and shear stiffness begin to influence the design, the number of active buckling modes may decrease.

In some cases a designer may wish to tailor the buckling response of a panel. For example, he may want only one buckling mode to be active at the design load, or he may want to put a substantial margin of safety on the buckling load for a given wavelength. Because of its generality, the present procedure can be used to tailor the buckling response of a panel.

In order to obtain some insight into this tailoring capability, a heavily loaded hat-stiffened panel and a more lightly loaded hat-stiffened panel were considered. The design requirements for these two examples are as follows:

Hat-stiffened panel	N_x/L		t_2		d		Comments
	kPa	lbf/in^2	mm	in.	cm	in.	
Heavily loaded example	5520	800	1.12	0.044	Free	Free	20-percent margin on buckling for $\lambda \leq L/4$
Lightly loaded example	689	100	Free	Free	12.7	5.0	50-percent margin on buckling for $\lambda \geq L/3$

The buckling response for the heavily loaded example designed with a 20-percent margin on local buckling ($\lambda \leq L/4$) and the buckling response for the corresponding panel designed without the margin on local buckling are presented in figure 14. The panel designed with no margin on local buckling (the circular symbols) is buckling critical at four wavelengths: $\lambda = L$, $L/2$, $L/3$, and $L/20$. The 20-percent increase in the local buckling load is achieved with a 2.4-percent increase in the mass index. There are no stiffener spacing requirements in this example.

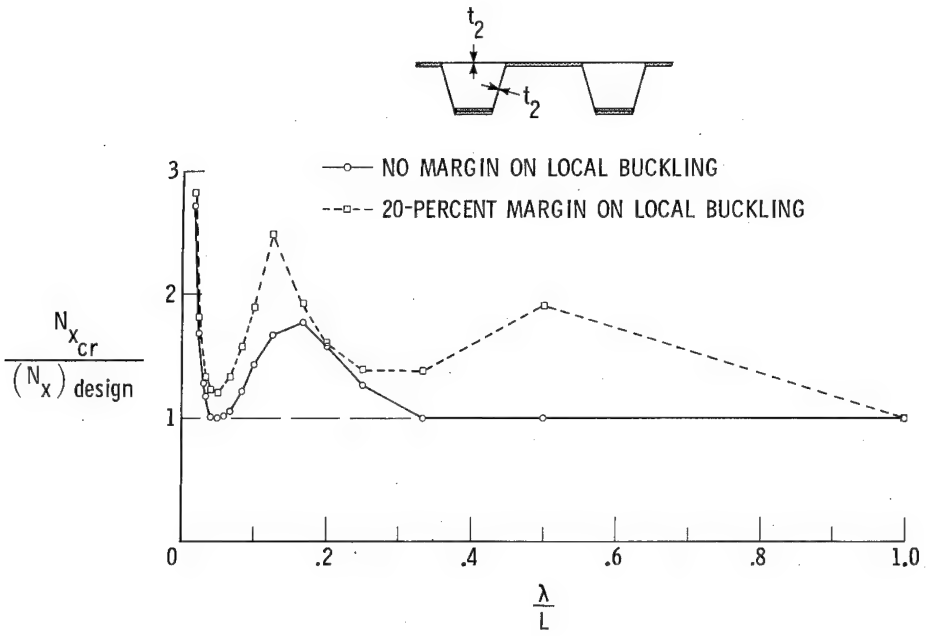

Figure 14.- Ratio of buckling load to design load as a function of buckling half-wavelength for two hat-stiffened panels designed for N_x/L = 5520 kPa (800 lbf/in^2); t_2 = 1.12 mm (0.044 in.).

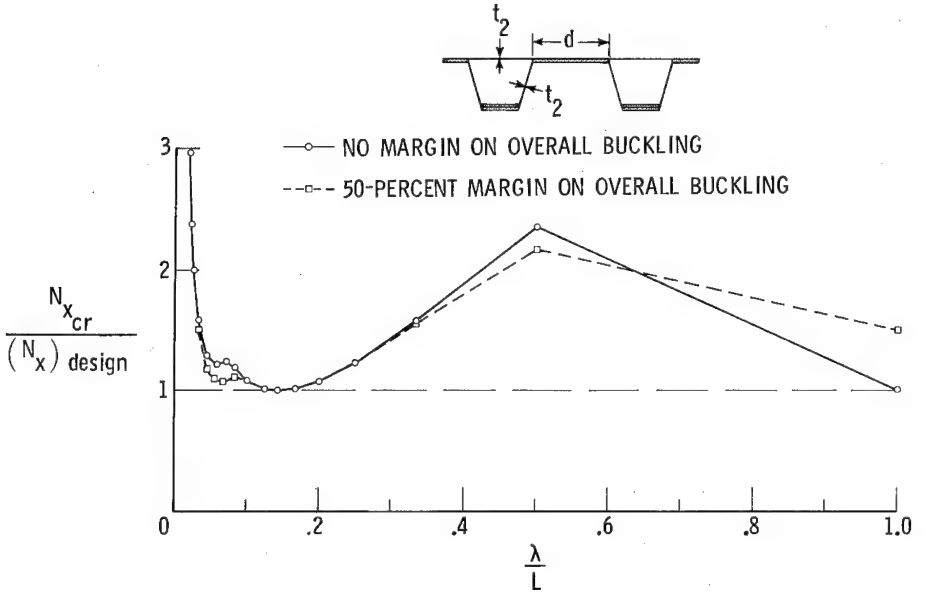

Figure 15.- Ratio of buckling load to design load as a function of buckling half-wavelength for two hat-stiffened panels designed for N_x/L = 689 kPa (100 lbf/in^2); d = 12.7 cm (5.0 in.).

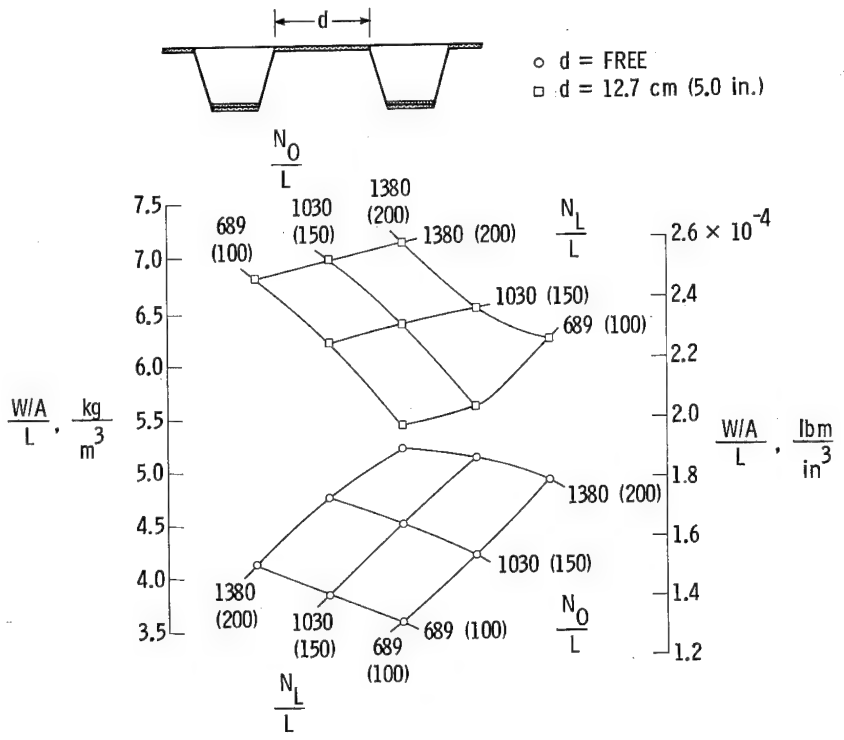

Figure 16.- Mass index as a function of required local buckling load N_L/L and required overall buckling load N_O/L for graphite-epoxy, hat-stiffened panels with and without design requirements on distance d between stiffeners. Required buckling loads given in kPa (lbf/in^2).

The buckling response for the more lightly loaded example designed with a 50-percent margin on overall buckling ($\lambda \geq L/3$) and the buckling response for the corresponding panel designed without the margin on overall buckling are presented in figure 15. Because of the stiffener spacing requirement, the local buckling wavelength for each of these panels is larger than for panels without that additional requirement. The 50-percent increase in the overall buckling load is achieved with a 3.2-percent increase in the mass index.

Additional studies were carried out with the more lightly loaded panel – both with and without a requirement on the stiffener spacing d. In these studies the mass penalty associated with increasing the local and/or overall buckling loads is examined. The results are presented in the form of carpet plots in figure 16. The stiffener spacing d is equal to 12.7 cm (5.0 in.) in the upper plot and varies freely in the lower plot. The quantities that are varied in the carpet plots are the required local buckling load $\left(N_L/L,\ \lambda \leq L/4\right)$ and the required overall buckling load $\left(N_O/L,\ \lambda \geq L/3\right)$. The vertical axis is the mass index $\frac{W/A}{L}$. The thickness t_2 varies freely.

All of these tailoring studies indicate that if a stiffened panel has no stiffener-spacing requirement, the local buckling load can be increased with a relatively small mass penalty. If, on the other hand, a stiffened panel has a stiffener-spacing requirement

that has a strong effect on the design, as it does in this case (see fig. 11), then the overall buckling load can be increased with a relatively small mass penalty.

Although imperfections are not considered in this report, it is known that imperfections can cause a substantial reduction in the buckling load of a panel. In many cases the reduction is caused by an interaction between imperfections and various possible buckling modes. Wavelengths of both imperfections and buckling loads are important. If a designer knows the type of imperfection that will occur during fabrication and/or the type of damage that is likely to occur during service, he may be able to tailor the buckling response of a panel to reduce the detrimental effects of the imperfections.

CONCLUDING REMARKS

A procedure is described for designing uniaxially stiffened panels made of composite material and subjected to combined inplane loads. The procedure uses a rigorous buckling analysis and nonlinear mathematical programing techniques. Computation efficiency is attained by using approximate analysis techniques based on Taylor series expansions. The procedure is very general and is applicable to panels with arbitrary cross sections. The procedure has been applied in a computer program for designing hat-stiffened and corrugated panels.

Design studies, all of which consider graphite-epoxy panels, are also presented. In one set of studies, generalized mass-strength charts are developed for hat-stiffened and corrugated panels subjected to combined longitudinal compression and shear. For the hat-stiffened panels, the procedure provides designs that are up to 14 percent lighter than those obtained with a previously published procedure based on a simplified buckling analysis. For the corrugated panels, the studies show that buckling modes involving torsional rolling may cause the simplified procedure to be unconservative. Buckling modes involving torsional rolling are treated accurately in the present procedure.

In other studies, the effects of combined longitudinal and transverse compression are investigated for hat-stiffened panels. Small transverse compressive loads severely reduce the load-carrying capacity of longitudinally stiffened panels. For transverse loads about one-tenth of longitudinal loads, panel mass must be increased by as much as 70 percent above the mass of panels with no transverse load.

Finally, the capability to tailor the buckling response of hat-stiffened panels under uniaxial compression is explored. Results indicate that relatively small mass increases could be associated with putting large margins on either (a) local buckling if no stiffener-spacing requirement is imposed, or (b) overall buckling if a minimum stiffener-spacing requirement is imposed. Carpet plots are presented for a limited loading range to

suggest mass penalties associated with buckling-response tailoring for panels with and without stiffener-spacing constraints.

The present study demonstrates that a panel design procedure with a high-quality buckling analysis and with complete generality of constraints is practical. Such procedures can be used to avoid failure from complex buckling modes and to determine mass and proportions of panels for multiple design load conditions and constraints.

Langley Research Center
National Aeronautics and Space Administration
Hampton, VA 23665
March 24, 1977

APPENDIX A

THE VIPASA ANALYSIS CODE

This appendix gives a brief description of the VIPASA analysis code in terms of the analysis-design procedure and examples presented herein. Two main topics are considered: (1) a general discussion of VIPASA with emphasis on structural modeling, and (2) conservatism in the VIPASA buckling analysis in the case of a shear loading and/or anisotropy. A more complete description of VIPASA is given in references 3, 4, and 12.

General Discussion of VIPASA

The computer program VIPASA calculates the buckling loads of structures comprised of flat rectangular plate elements connected together along their longitudinal edges. The response of each element is obtained using an exact solution of the thin-plate equations with anisotropic terms included. The analysis connects the individual plate elements and maintains continuity of the buckle pattern across the intersection of neighboring plate elements. Individual plate elements may be isotropic, orthotropic, or anisotropic. The only limitations are that the plates must be uniform along their length and that the plate laminates must not exhibit bending-stretching coupling or stretching-shearing coupling. (Bending-twisting coupling is allowed.) Laminates that are midplane symmetric and balanced satisfy these requirements. The structure may be subjected to any combination of longitudinal, transverse, and shear loads that are constant along the length.

In the VIPASA analysis, a local coordinate system is defined for each individual plate element. An example is shown in figure 17. The X, Y_ℓ, Z_ℓ axes define the local coordinate system in the local longitudinal, transverse, and lateral directions, respectively. The buckling displacements u, v, and w are defined in this local coordinate system and are also shown in figure 17. The X, Y, Z axes denote the overall-panel coordinate system.

In VIPASA, the buckling boundary conditions along the edges $x = 0$ and $x = L$ (fig. 18) are always simple support – that is, u is unrestrained, $v = w = 0$, and $w_{,x}$ is unrestrained. The unconnected longitudinal edges may, however, have various boundary conditions. In the examples presented in this report, the boundary conditions along the unconnected longitudinal edges are either simple support or symmetric. (Calculations were made with both boundary conditions.) Symmetric boundary conditions along the unconnected longitudinal edges are defined as u is unrestrained, $v = 0$, w is unrestrained, and $w_{,y_\ell} = 0$. The net effect of the individual plate-element boundary conditions is to produce identical u,v,w boundary conditions in the X, Y, Z, respectively, coordinate system associated with the overall panel.

APPENDIX A

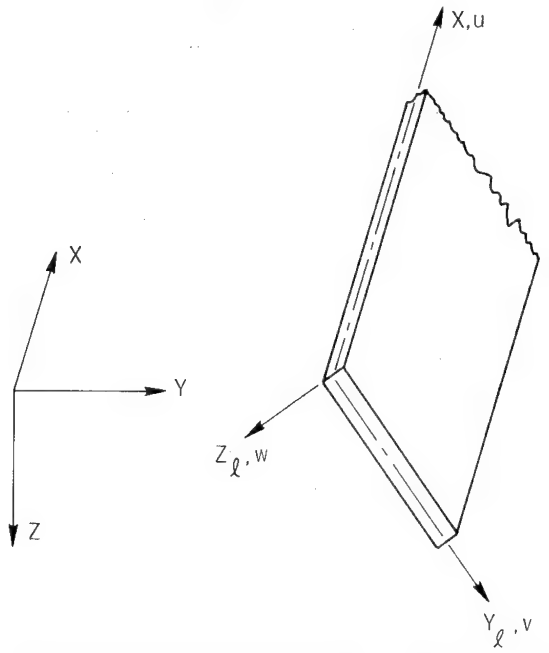

Figure 17.- Local coordinate system for panel element and overall coordinate system for stiffened panel.

In the VIPASA model for the hat-stiffened and corrugated panels considered in this report, one stiffener section is idealized as an assemblage of flat plates, then eight of these substructures are joined together for the final model. A sample cross section is shown in figure 18. Because eight stiffeners are used to model all of the panels discussed

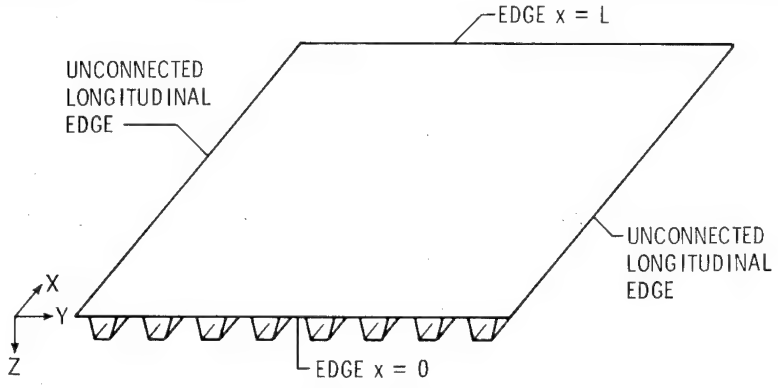

Figure 18.- Eight-stiffener mathematical model of hat-stiffened panel.

in this report, symmetric and simple support boundary conditions along the unconnected longitudinal edges give virtually identical values for the buckling load. The potential for buckle widths (y-direction) to extend across more than eight stiffeners increases with the presence of shear loadings and that potential is even greater for transverse loadings. In the results presented in figures 9 and 13, checks were made at a few design points to insure that eight stiffeners were adequate and that the minimum buckling load had been found.

APPENDIX A

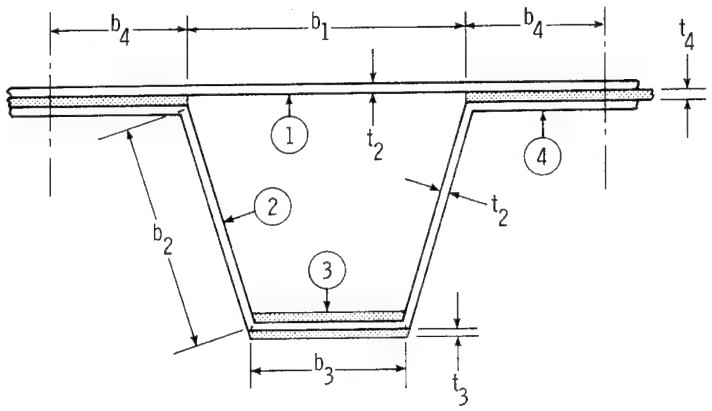

(a) Approximate physical model.

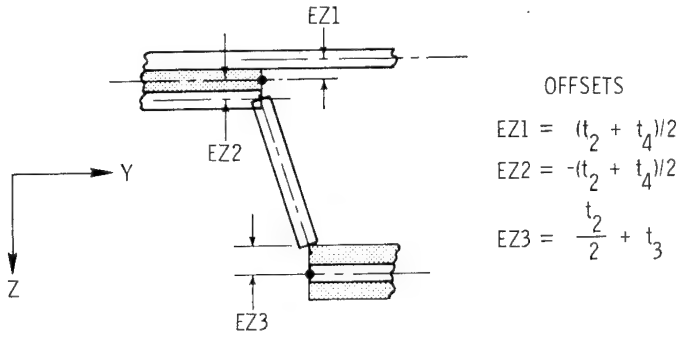

(b) Mathematical model used in VIPASA.

Figure 19.- Approximate physical model for hat-stiffened panel and corresponding mathematical model used by VIPASA.

A detailed model of one repeating section of a hat-stiffened panel is shown in figure 19(a). Values for plate stiffnesses supplied to VIPASA are based on the fact that adjacent elements are connected through nodes at the element center lines. When plates do not align center line to center line, which is the case in figure 19(a), eccentricities or offsets must be supplied to VIPASA in order for the panel to have the proper stiffnesses. The eccentric connections for the hat-stiffened panel are illustrated in figure 19(b). The nodes are indicated by dots, and the offset distances EZ1, EZ2, and EZ3 represent eccentricities in the z-direction. Element 1 is given a positive offset EZ1 so that the top surface of the panel is continuous and flat through its width. At the juncture of element 2 with element 4, element 2 is given a negative eccentricity EZ2. Where element 2 joins element 3, element 2 is given a positive eccentricity EZ3. The sign convention used in figure 19(b) is consistent with that used in VIPASA.

Conservative Analysis in the Case of Shear Loading and/or Anisotropy

In order to obtain an exact solution to the panel buckling problem, the following buckling mode shape is assumed in the VIPASA analysis for each plate element:

APPENDIX A

$$W = \mathrm{Re}\left(F(y_\ell)\, e^{\frac{i\pi x}{\lambda}}\right) \tag{A1}$$

For orthotropic plates without shear loading, F is real and, hence, node lines are straight, perpendicular to the x-direction, and spaced λ apart. In this case, simple support boundary conditions are achieved at the boundaries $x = 0$ and $x = L$. With shear and/or anisotropy present, F is complex and node lines are skewed and not straight, but they are still spaced λ apart. An example is shown in figure 20. If λ is

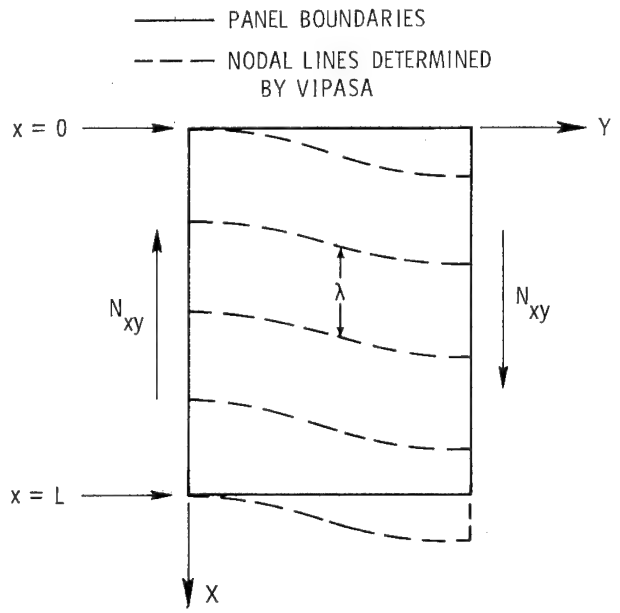

Figure 20.- Nodal lines determined by VIPASA in the case of a shear loading and/or anisotropy.

small compared with panel length, the unrestrained buckle pattern can develop in the central region of the panel. The VIPASA results are, in this case, sufficiently accurate. As λ approaches L, the VIPASA results can be quite conservative. The reason is as follows. As can be seen in figure 20, the skewed nodal lines do not coincide with the panel edges $x = 0$ and $x = L$. The additional constraint arising from the requirement that the nodal lines at $x = 0$ and $x = L$ coincide with the panel edges results in long-wavelength buckling loads that are, in many cases, appreciably higher than those determined by VIPASA, where the nodal lines are not required to conform with the edges. Calculations have shown that for long-wavelength buckling modes the effect of anisotropy is minimal. Anisotropy, therefore, causes negligible conservatism in a VIPASA analysis. The presence of a shear loading can, however, lead to very conservative results for λ equal to L.

Because of VIPASA's conservatism in the case of long-wavelength buckling if a shear load is present, a modified analysis procedure is used for the case $\lambda = L$. The

modified analysis is based on an interaction formula used in reference 11. In the case of a combined longitudinal and shear loading $\left(N_x \text{ and } N_{xy}\right)$ the loading is considered to be critical if

$$\frac{N_x}{N_{x_{cr}}} + \left(\frac{N_{xy}}{N_{xy_{cr}}}\right)^2 = 1 \tag{A2}$$

The critical longitudinal compressive load $N_{x_{cr}}$ is calculated with VIPASA. The critical shear load $N_{xy_{cr}}$ is calculated using smeared orthotropic theory which is the same approach used in reference 11. It is emphasized that this modified analysis procedure is used only for the case $\lambda = L$.

APPENDIX B

TESTING THE ADEQUACY OF THE SIMPLIFIED ANALYSIS-DESIGN PROCEDURE OF NASA TN D-8257

In NASA TN D-8257, two forms of buckling are postulated. One form is an overall mode, and the other form is a local mode. Buckling of the panel is assumed to be prevented if these two forms of buckling are prevented.

In the overall buckling mode, the panel is assumed to buckle as a wide column. All the orthotropic stiffnesses are smeared. This failure mode is often referred to as Euler buckling. In the local buckling mode, each element of the panel cross section is treated as a narrow orthotropic plate that is simply supported along its lines of attachment to adjacent elements. Buckling of each element is treated separately (i.e., one can speak of buckling of element 1, buckling of element 2, etc.). This approach to local buckling ignores continuity of buckling-mode shape. The advantage of this type of analysis procedure is that closed-form solutions exist for the buckling modes that are postulated. The disadvantage is that some buckling modes – in particular those involving joint displacement (rolling modes, for example) – are not considered. The analysis approach used in reference 11 is a traditional approach that has been used in many other panel optimization procedures.

In contrast with the simplified analysis of reference 11, the VIPASA analysis code provides a high-quality buckling analysis that considers all buckling modes and insures continuity of the buckling pattern across the intersection of neighboring plate elements. Anisotropy in the element bending stiffnesses can also be taken into account. The major known shortcoming of the VIPASA code is the skewed boundary node lines (rather than straight boundary node lines) determined by VIPASA in the case of a shear loading and/or anisotropy. That characteristic and a modification to the analysis are discussed in appendix A.

In this appendix the adequacy of the analysis-design procedure of reference 11, including the orthotropic assumption, is checked using the present procedure. The checking is done with two levels of analysis. First, designs obtained with the procedure of reference 11 are analyzed with VIPASA under the assumption of orthotropy. In these cases differences in buckling loads cannot be ascribed to anisotropic effects. Second, the same designs are analyzed with VIPASA using the anisotropic stiffnesses D_{16} and D_{26} which couple bending behavior with torsional behavior. (See, for example, eq. (A1) in ref. 11.) Finally, the masses of the panels designed using the procedure of reference 11 are compared with the masses of panels designed using the present procedure.

APPENDIX B

The analysis and design comparisons that are presented in table III fall under two main headings: "Analysis Comparisons" and "Design Comparisons." Each of these headings is subdivided into two subheadings depending upon the analysis used in VIPASA. In the analysis comparisons, the data presented are the ratios of the buckling load calculated by VIPASA to the buckling load calculated using the procedure of reference 11. The panels being analyzed were designed using the procedure of reference 11; therefore, the buckling load calculated by the procedure of reference 11 is the design load. The buckling half-wavelength λ determined by VIPASA is also presented. In the design comparisons, the data presented are the ratios of the mass index of panels designed using the present procedure to the mass index of panels designed using the procedure of reference 11.

Hat-Stiffened Panels

Longitudinal compression N_x.- Five hat-stiffened panels that were designed using the procedure of reference 11 to support longitudinal compressive loads N_x were analyzed with VIPASA. Panels were also designed using the present procedure so that panel masses could be compared. The results are summarized in table III.

More valuable information on the buckling characteristics, including the anisotropic effect, can be obtained by examining the buckling response over a range of buckling wavelengths. A buckling response diagram obtained with the VIPASA code for a hat-stiffened panel having t_2 = 0.56 mm (0.022 in.) and designed with the procedure of reference 11 for a loading of N_x/L = 689 kPa (100 lbf/in^2) is presented in figure 21. The circular

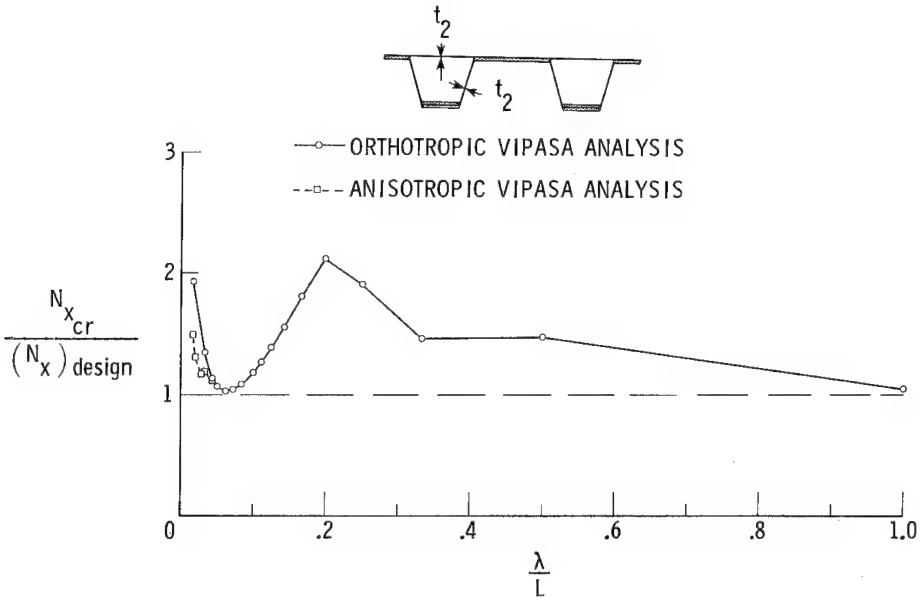

Figure 21.- Ratio of buckling load to design load as a function of buckling half-wavelength for a hat-stiffened panel designed using the procedure of reference 11 for a loading of of N_x/L = 689 kPa (100 lbf/in^2); t_2 = 0.56 mm (0.022 in.).

symbols indicate the calculated buckling loads for a given half-wavelength obtained using an orthotropic VIPASA analysis. The square symbols are for a VIPASA analysis including anisotropic D_{16} and D_{26} terms. The critical overall buckling load occurs at $\lambda = L$, and the critical local buckling load occurs at $\lambda = L/16$. The buckling mode shapes for these two values of λ are similar to those presented in figures 6 and 7, respectively. The main difference is that in the panel of figure 21 the local buckling mode does not involve deformation of the hat cap (element 3 in fig. 8).

Three conclusions can be drawn from the results presented in figure 21 and from the first set of studies in table III. First, for the cases examined, anisotropy has its main effect on buckling modes with wavelengths less than the critical wavelengths for local buckling. Therefore, for these cases, anisotropy has little impact on the buckling load for longitudinal compressive loadings. Second, the simplified analysis of reference 11 appears to be adequate[1] for hat-stiffened panels loaded by longitudinal compression. However, it would be inadequate if the wavelengths for local buckling and strong anisotropic effects coincide. (Calculations indicate that the D_{16} and D_{26} terms for elements 1 and 2 of fig. 8 provide almost all of the anisotropic effects for the short-wavelength buckle modes.) Third, for hat-stiffened panels with a longitudinal compressive loading N_x, mass savings on the order of 2 to 9 percent are possible with the present design procedure.

Longitudinal compression and shear N_x and N_{xy}.- Three hat-stiffened panels that were designed using the procedure of reference 11 to support longitudinal compressive and shear loads N_x and N_{xy} were analyzed with VIPASA. Panels were also designed using the present procedure so that panel masses could be compared. The results are summarized in table III. The positive and negative values of N_{xy}/N_x indicate the sign of the shear loading N_{xy}. Because the analysis of reference 11 is based on orthotropic theory, it cannot distinguish between positive and negative values of N_{xy}. In contrast, since VIPASA can take into account the anisotropic D_{16} and D_{26} terms VIPASA can distinguish between positive and negative values of N_{xy}.[2] In some cases presented in table III, the anisotropic effects are large. Panels designed with an orthotropic analysis can have an anisotropic buckling load substantially less for a negative value of N_{xy} than for a positive value of N_{xy}. Also, the mass of a panel designed for a negative value

[1]As used here and elsewhere in this appendix, the word "adequate" means that the panels designed using the procedure of reference 11 do not buckle when analyzed using the VIPASA code. In many cases the more sophisticated analysis-design procedure presented herein provides designs that are substantially lighter than designs obtained with the procedure of reference 11.

[2]The effect of a sign change for N_{xy} is the same as the effect of changing the sign of the D_{16} and D_{26} terms. Positive values of D_{16} and D_{26} are used in all the results presented.

of N_{xy} can be substantially greater than the mass of a panel designed for a positive value of N_{xy}.

A buckling response diagram provides a clearer picture of the buckling characteristics including local buckling and anisotropic effects. The buckling response diagrams for the panel designed for N_x/L = 689 kPa (100 lbf/in^2), $N_{xy}/N_x = 0.1$ and for the panel designed for N_x/L = 207 kPa (30 lbf/in^2), $N_{xy}/N_x = 1.0$ are presented in figures 22 and 23, respectively. Both panels were designed with the procedure of reference 11. The circular symbols are for a VIPASA analysis that assumes complete orthotropy. The square and triangular symbols are for VIPASA analyses that account for D_{16} and D_{26} terms. The square symbols indicate positive values of N_{xy} and the triangular symbols indicate negative values. The solid symbol at $\lambda = L$ is for the modified analysis described in appendix A. (See eq. (A2).)

Considering first the orthotropic VIPASA analysis indicated by the circular symbols, the analysis of reference 11 is adequate for the short-wavelength buckles. However, when the VIPASA analysis includes the D_{16} and D_{26} terms there is a substantial difference in the short-wavelength buckling loads depending on the sign of the shear loading. These effects cannot be detected with the analysis of reference 11.

It can be concluded that for combined longitudinal compression and shear loadings the local buckling analysis in reference 11 is adequate for hat-stiffened panels made up of orthotropic elements. When anisotropic effects are large, as they can be in a four-ply laminate, the analysis of reference 11 is inadequate, and a modified local buckling analysis that accounts for anisotropic effects must be used.

An analysis similar to that of reference 11 which takes into account the effects of the D_{16} and D_{26} terms in the local buckling analysis for elements 1 and 2 is easily developed. The technique can be used if the thickness t_2 is fixed during the synthesis. With t_2 fixed, the D_{ij} matrix shared by elements 1 and 2 is fixed. The local buckling loads of elements 1 and 2 can, therefore, be expressed as

$$\left(N_{x_{cr}}\right)_k = \frac{C}{(b_k)^2} \tag{B1}$$

$$\left(N_{xy_{cr}}\right)_k = \frac{K}{(b_k)^2} \tag{B2}$$

where b_k is the width of element k, and C and K are constants, each of which can be determined by carrying out a single anisotropic buckling analysis with a code such as VIPASA. Sample calculations indicate that the resulting analysis produces conservative results for hat-stiffened panels.

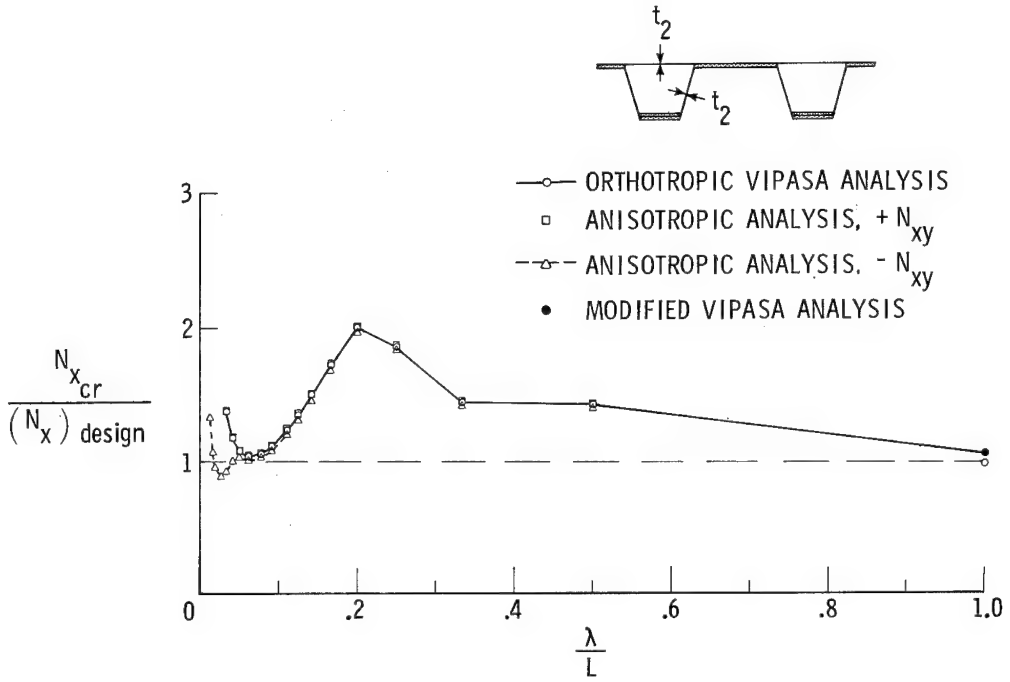

Figure 22.- Ratio of buckling load to design load as a function of buckling half-wavelength for a hat-stiffened panel designed using the procedure of reference 11 for a loading of N_x/L = 689 kPa (100 lbf/in^2); N_{xy}/N_x = 0.1; t_2 = 0.56 mm (0.022 in.).

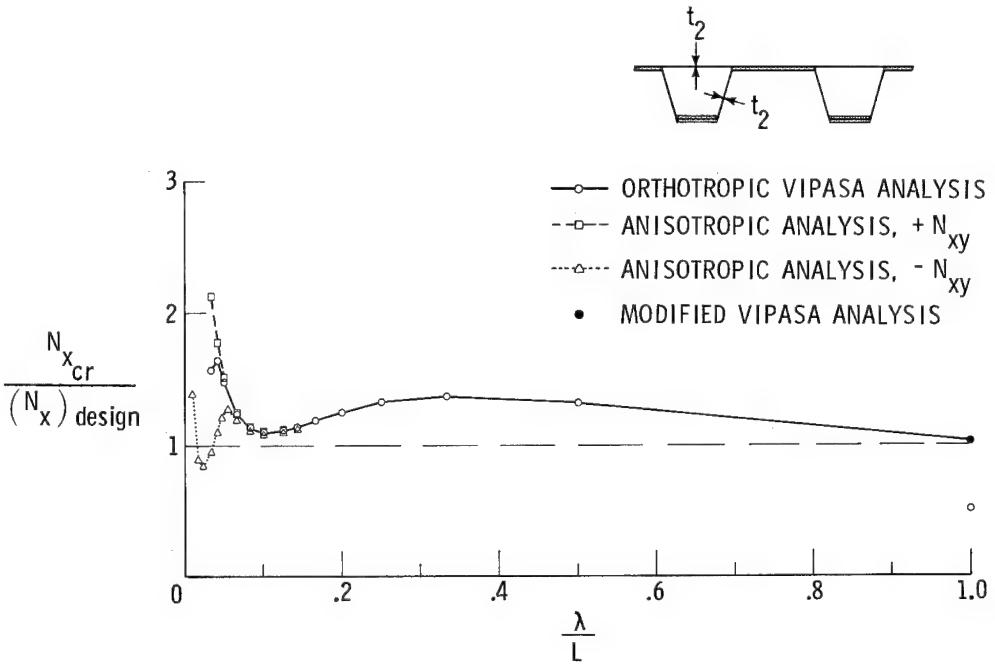

Figure 23.- Ratio of buckling load to design load as a function of buckling half-wavelength for a hat-stiffened panel designed using the procedure of reference 11 for a loading of N_x/L = 207 kPa (30 lbf/in^2); N_{xy}/N_x = 1.0; t_2 = 0.56 mm (0.022 in.).

APPENDIX B

Corrugated Panels

Longitudinal compression N_x.- Five corrugated panels that were designed using the procedure of reference 11 to support longitudinal compressive loads N_x were analyzed using VIPASA. Panels were also designed using the present procedure so that panel masses could be compared. The results are presented in table III and figures 24 and 25.

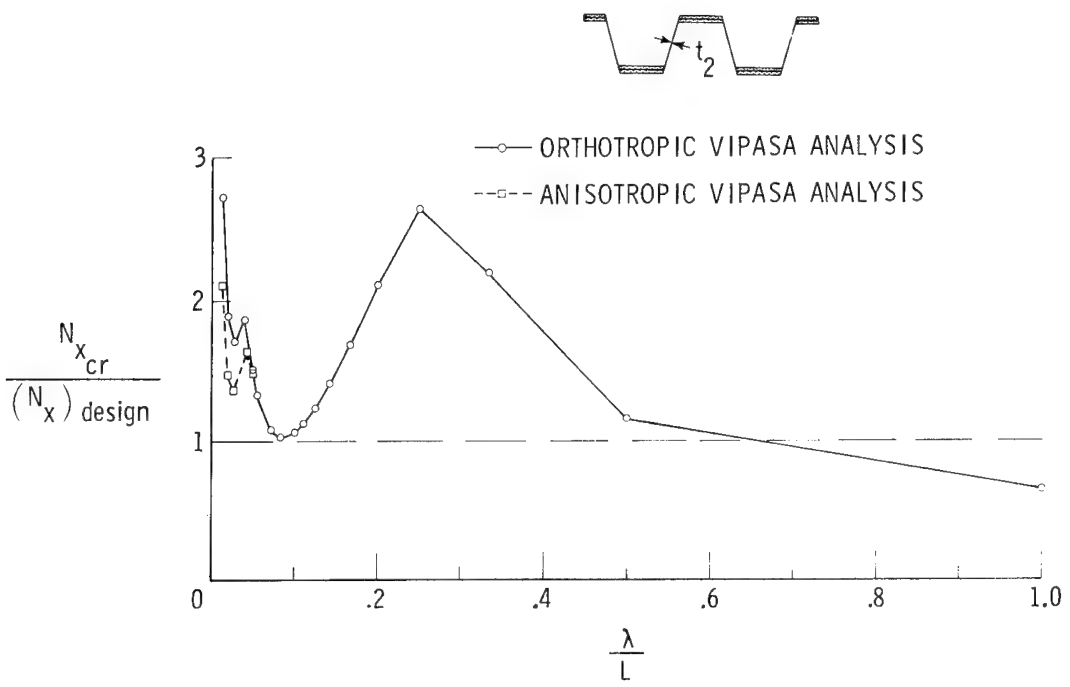

Figure 24.- Ratio of buckling load to design load as a function of buckling half-wavelength for a corrugated panel designed using the procedure of reference 11 for a loading of N_x/L = 1380 kPa (200 lbf/in^2); t_2 = 0.56 mm (0.022 in.).

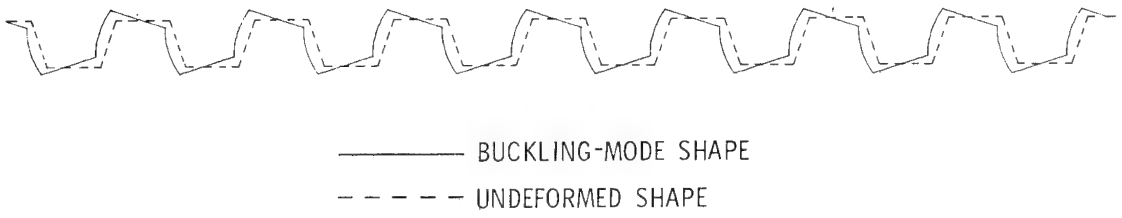

Figure 25.- Buckling-mode shape for panel whose buckling response diagram is shown in figure 24.

APPENDIX B

It can be seen in table III that deficiencies in the simplified analysis of reference 11 exist for this configuration even when comparisons are made between orthotropic analyses. The analysis of reference 11 appears to be adequate in the lightly loaded region of a given thickness t_2, but is very unconservative in the heavily loaded region of a given thickness. (These regions can be seen in fig. 19 of ref. 11.) The buckling response diagram for the panel designed for $N_x/L = 1380$ kPa (200 lbf/in^2) with $t_2 = 0.56$ mm (0.022 in.) is presented in figure 24. The buckling mode shape for the $\lambda = L$ buckling mode of that panel is presented in figure 25. Although the simplified (ref. 11) analysis for compression buckling of corrugated panels appears to be adequate for short-wavelength buckling, it is not adequate for the longer wavelength buckling $\lambda = L$ and $L/2$ where, according to the buckling-mode shape presented in figure 25, the corrugated stiffeners are rolling or twisting. Twisting modes cannot be predicted by the analysis of reference 11. As in the hat-stiffened panel, anisotropic effects are small in the case of corrugated panels loaded only in longitudinal compression.

Longitudinal compression and shear N_x and N_{xy}.- Two corrugated panels designed using the procedure of reference 11 to support longitudinal compressive and shear loads N_x and N_{xy} were analyzed using VIPASA. Panels were also designed using the present procedure so that panel masses could be compared. The results are summarized in table III and figure 26.

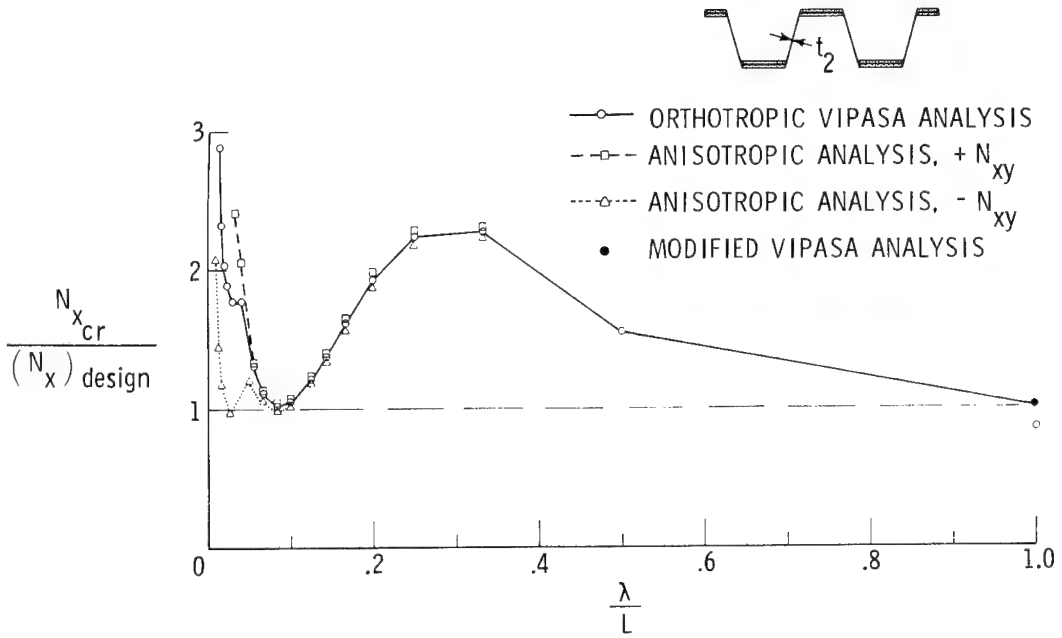

Figure 26.- Ratio of buckling load to design load as a function of buckling half-wavelength for a corrugated panel designed using the procedure of reference 11 for a loading of $N_x/L = 689$ kPa (100 lbf/in^2); $N_{xy}/N_x = 0.1$; $t_2 = 0.56$ mm (0.022 in.).

APPENDIX B

The buckling response diagram obtained with the VIPASA code for the $t_2 = 0.56$ mm (0.022 in.) panel designed with the reference 11 analysis for a loading of $N_x/L = 689$ kPa (100 lbf/in^2), $N_{xy}/N_x = 0.1$ is presented in figure 26. The figure indicates that the simplified analysis would be adequate for this corrugated panel if it were made up of orthotropic elements. As in the case of the hat-stiffened panel, anisotropy affects mainly the short-wavelength buckling loads.

REFERENCES

1. Peterson, James P.: Structural Efficiency of Aluminum Multiweb Beams and Z-Stiffened Panels Reinforced With Filamentary Boron-Epoxy Composite. NASA TN D-5856, 1970.

2. Williams, Jerry G.; and Stein, Manuel: Buckling Behavior and Structural Efficiency of Open-Section Stiffened Composite Compression Panels. AIAA J., vol. 14, no. 11, Nov. 1976, pp. 1618-1626.

3. Wittrick, W. H.; and Williams, F. W.: Buckling and Vibration of Anisotropic or Isotropic Plate Assemblies Under Combined Loadings. Int. J. Mech. Sci., vol. 16, no. 4, Apr. 1974, pp. 209-239.

4. Plank, R. J.; and Williams, F. W.: Critical Buckling of Some Stiffened Panels in Compression, Shear and Bending. Aeronaut. Q., vol. XXV, pt. 3, Aug. 1974, pp. 165-179.

5. Tripp, L. L.; Tamekuni, M.; and Viswanathan, A. V.: User's Manual – BUCLASP 2: A Computer Program for Instability Analysis of Biaxially Loaded Composite Stiffened Panels and Other Structures. NASA CR-112226, 1973.

6. Viswanathan, A. V.; and Tamekuni, M.: Elastic Buckling Analysis for Composite Stiffened Panels and Other Structures Subjected to Biaxial Inplane Loads. NASA CR-2216, 1973.

7. Schmit, L. A., Jr.; and Farshi, B.: Some Approximation Concepts for Structural Synthesis. AIAA J., vol. 12, no. 5, May 1974, pp. 692-699.

8. Schmit, Lucien A., Jr.; and Miura, Hirokazu: Approximation Concepts for Efficient Structural Synthesis. NASA CR-2552, 1976.

9. Haftka, Raphael T.: Automated Procedure for Design of Wing Structures To Satisfy Strength and Flutter Requirements. NASA TN D-7264, 1973.

10. Vanderplaats, Garret N.: CONMIN – A Fortran Program for Constrained Function Minimization. User's Manual. NASA TM X-62,282, 1973.

11. Stroud, W. Jefferson; and Agranoff, Nancy: Minimum-Mass Design of Filamentary Composite Panels Under Combined Loads: Design Procedure Based on Simplified Buckling Equations. NASA TN D-8257, 1976.

12. Anderson, Melvin S.; Hennessy, Katherine W.; and Heard, Walter L., Jr.: Addendum to Users Guide to VIPASA (Vibration and Instability of Plate Assemblies Including Shear and Anisotropy). NASA TM X-73914, 1976.

TABLE I.- LIMITS ON DESIGN VARIABLES

Dimension	Hat-stiffened panel		Corrugated panel	
	cm	in.	cm	in.
$t_3(0^o)$, minimum	0	0	0	0
$t_4(0^o)$, minimum	0	0	0	0
$t_3(0^o)$, maximum	0.318	0.125	0.318	0.125
$t_4(0^o)$, maximum	.635	.250	Not applicable	
b_1, minimum	2.03	.80	2.03	.80
b_2, minimum	1.02	.40	1.02	.40
b_3, minimum	2.03	.80	2.03	.80
b_4, minimum	1.02	.40	Not applicable	

TABLE II.- PROPERTIES OF GRAPHITE-EPOXY MATERIAL USED IN SAMPLE CALCULATIONS

[ten. denotes tension; comp. denotes compression]

Symbol	Value in SI Units	Value in U.S. Customary Units
Density and elastic properties		
ρ	1520 kg/m^3	0.055 lbm/in^3
E_1	145 GPa	21×10^6 psi
E_2	16.5 GPa	2.39×10^6 psi
G_{12}	4.48 GPa	0.65×10^6 psi
μ_{12}	0.314	0.314
μ_{21}	0.037	0.037
Allowable stresses		
σ_1^a (ten.)	1240 MPa	180 ksi
σ_1^a (comp.)	-1240 MPa	-180 ksi
σ_2^a (ten.)	55.2 MPa	8 ksi
σ_2^a (comp.)	-207 MPa	-30 ksi
τ_{12}^a	82.7 MPa	12 ksi
Allowable strains		
ϵ_1^a (ten.)	0.0087	0.0087
ϵ_1^a (comp.)	-0.0087	-0.0087
ϵ_2^a (ten.)	0.00475	0.00475
ϵ_2^a (comp.)	-0.01764	-0.01764
γ_{12}^a	0.01846	0.01846

TABLE III.- RATIOS OF BUCKLING LOADS AND MASS INDICES FOR GRAPHITE-EPOXY PANELS ANALYZED AND DESIGNED BY PROCEDURE OF REFERENCE 11 AND BY PRESENT PROCEDURE

Design loading			$t_2(\pm 45^o)$		Analysis comparisons[1] $\frac{\left(N_{x_{cr}}\right)_{VIPASA}}{\left(N_{x_{cr}}\right)_{reference\ 11}}$		Design comparisons $\frac{\left(\frac{W/A}{L}\right)_{present\ procedure}}{\left(\frac{W/A}{L}\right)_{reference\ 11}}$	
$\frac{N_x}{L}$ kPa	$\frac{N_x}{L}$ $\frac{lbf}{in^2}$	$\frac{N_{xy}}{N_x}$	cm	in.	VIPASA orthotropic	VIPASA anisotropic	Present procedure orthotropic	Present procedure anisotropic
Hat-stiffened panels, N_x								
345	50	0	0.056	0.022	1.04 $\lambda = L$	1.03 $\lambda = L/14$	0.97	0.98
689	100	0	.056	.022	1.03 $\lambda = L/16$	1.02 $\lambda = L/16$	.95	.97
1380	200	0	.056	.022	1.01 $\lambda = L$	1.01 $\lambda = L$	.91	.96
2070	300	0	.056	.022	.98 $\lambda = L/2$	.98 $\lambda = L/2$	.96	.98
2070	300	0	.112	.044	1.00 $\lambda = L$		.97	
Hat-stiffened panels, N_x and N_{xy}								
689	100	+0.1	0.056	0.022	1.04 $\lambda = L/16$	1.05 $\lambda = L/16$	0.93	0.93
		-.1				.89 $\lambda = L/38$		1.00
1380	200	+.1	.056	.022	1.02 $\lambda = L/12$	1.03 $\lambda = L/12$	.94	.92
		-.1				1.01 $\lambda = L/12$		.98
207	30	+1.0	.056	.022	1.03 $\lambda = L$	1.03 $\lambda = L$	.85	.83
		-1.0				.84 $\lambda = L/43$		1.46
Corrugated panels, N_x								
345	50	0	0.056	0.022	1.03 $\lambda = L$	1.00 $\lambda = L/19$	0.96	0.98
689	100	0	.056	.022	.96 $\lambda = L/2$	.96 $\lambda = L/2$	1.00	1.01
1380	200	0	.056	.022	.66 $\lambda = L$	.66 $\lambda = L$	.97	.98
2760	400	0	.056	.022	.57 $\lambda = L$	.57 $\lambda = L$	1.11	1.13
1380	200	0	.112	.044	.82 $\lambda = L/2$		1.06	
Corrugated panels, N_x and N_{xy}								
345	50	+0.1	0.056	0.022	1.03 $\lambda = L$	1.03 $\lambda = L$	0.96	0.92
		-.1				.90 $\lambda = L/29$		1.02
689	100	+.1	.056	.022	1.00 $\lambda = L$	1.00 $\lambda = L$	.86	.84
		-.1				.97 $\lambda = L/38$		1.01

[1]Designs obtained with procedure of reference 11.

"The aeronautical and space activities of the United States shall be conducted so as to contribute . . . to the expansion of human knowledge of phenomena in the atmosphere and space. The Administration shall provide for the widest practicable and appropriate dissemination of information concerning its activities and the results thereof."

—NATIONAL AERONAUTICS AND SPACE ACT OF 1958

NASA SCIENTIFIC AND TECHNICAL PUBLICATIONS

TECHNICAL REPORTS: Scientific and technical information considered important, complete, and a lasting contribution to existing knowledge.

TECHNICAL NOTES: Information less broad in scope but nevertheless of importance as a contribution to existing knowledge.

TECHNICAL MEMORANDUMS: Information receiving limited distribution because of preliminary data, security classification, or other reasons. Also includes conference proceedings with either limited or unlimited distribution.

CONTRACTOR REPORTS: Scientific and technical information generated under a NASA contract or grant and considered an important contribution to existing knowledge.

TECHNICAL TRANSLATIONS: Information published in a foreign language considered to merit NASA distribution in English.

SPECIAL PUBLICATIONS: Information derived from or of value to NASA activities. Publications include final reports of major projects, monographs, data compilations, handbooks, sourcebooks, and special bibliographies.

TECHNOLOGY UTILIZATION PUBLICATIONS: Information on technology used by NASA that may be of particular interest in commercial and other non-aerospace applications. Publications include Tech Briefs, Technology Utilization Reports and Technology Surveys.

Details on the availability of these publications may be obtained from:

SCIENTIFIC AND TECHNICAL INFORMATION OFFICE

NATIONAL AERONAUTICS AND SPACE ADMINISTRATION

Washington, D.C. 20546